PHYSICAL REVIEW B
CONDENSED MATTER

THIRD SERIES, VOLUME 27, NUMBER 3 1 FEBRUARY 1983

Valence and delocalization of Yb in the Chevrel-phase $YbMo_6S_8$

J. D. Jorgensen, and D. G. Hinks
Solid State Science Division, Argonne National Laboratory, Argonne, Illinois 60439

D. R. Noakes
Solid State Science Division, Argonne National Laboratory, Argonne, Illinois 60439
and Physics Department, University of Chicago, Chicago, Illinois 60637

P. J. Viccaro* and G. K. Shenoy
Solid State Science Division, Argonne National Laboratory, Argonne, Illinois 60439

(Received 6 October 1982)

Mössbauer isomer-shift measurements show that Yb is divalent in $YbMo_6S_8$. The asymmetry of the Yb thermal vibration at 4.2 K obtained from the Goldanskii-Karyagin effect is much smaller than that obtained from a Rietveld refinement of neutron powder diffraction data at 16 K. This suggests that the displacement of Yb off the origin includes a significant, ~0.1-Å, static component which persists at low temperature. Full structural refinements at 16, 77, and 295 K show several interesting structural changes versus temperature.

I. INTRODUCTION

The valence and site of Yb in the Chevrel-phase compound $YbMo_6S_8$ have been subjects of controversy in recent literature. Fischer *et al.*[1] reported that both the magnetic susceptibility and lattice parameters indicated that their sample of beginning stoichiometry $Yb_{1.2}Mo_6S_8$ contained 0.94 Yb^{2+} and 0.26 Yb^{3+}. They speculated that only the Yb^{2+} occupied the site at the origin. A second sample showed 0.8 Yb^{2+} and 0.2 Yb^{3+}. Alekseevskii *et al.*[2] attributed a specific-heat anomaly in $YbMo_6S_8$ at ~2.7 K to the onset of ferromagnetic ordering and concluded that part of the Yb was present as Yb^{3+}. This same conclusion was drawn by Bonville *et al.*[3], who observed the same anomaly by the Mössbauer effect with measurements extending from 60 mK to 40 K. However, a later paper by Bonville *et al.*[4] concluded that the Yb^{3+} ions could be present in an oxysulfide impurity and not in $YbMo_6S_8$. Other recent work by Tarascon *et al.*[5] showed that when samples were prepared from high-purity materials under carefully controlled conditions, magnetic susceptibilities indicated no more than about 2.5% Yb^{3+}. These authors speculated that the Yb^{3+} ions which are smaller (0.87 Å) than Yb^{2+} ions (1.02 Å) could occupy the outer tetrahedral sites rather than the origin.

The metal ions M in the Chevrel phases $M_xMo_6S_8$, have been shown to occupy sites of two general types.[6] Large M ions (e.g., Sn, Pb, La, etc.) are located on the ternary axis at the origin in a site of $\bar{3}$-point-group symmetry in space group $R\bar{3}$ (Fig. 1). Small ions (e.g., Cu, Fe, Ni, Co) occupy two sixfold sites of 1-point-group symmetry displaced from the origin in the direction of open channels extending along the rhombohedral axes. The possibility of both types of sites being occupied has been demonstrated by a recent structural refinement of $SnFe_{0.4}Mo_6S_8$ where Sn occupies the origin and Fe occupies an outer sixfold site.[7] Thus the proposal that a $YbMo_6S_8$ structure containing both Yb^{2+} and Yb^{3+} could have Yb^{2+} at the origin and Yb^{3+} in a sixfold site is not entirely illogical.

For structures with large ions at the origin the ion typically exhibits a strongly anisotropic thermal ellipsoid with large motion perpendicular to the threefold axis.[6,8] From structural refinements alone it is impossible to learn whether this displacement is static or dynamic. The displacement undoubtedly arises because the two axial chalcogen atoms are too close for comfortable occupation of the origin.

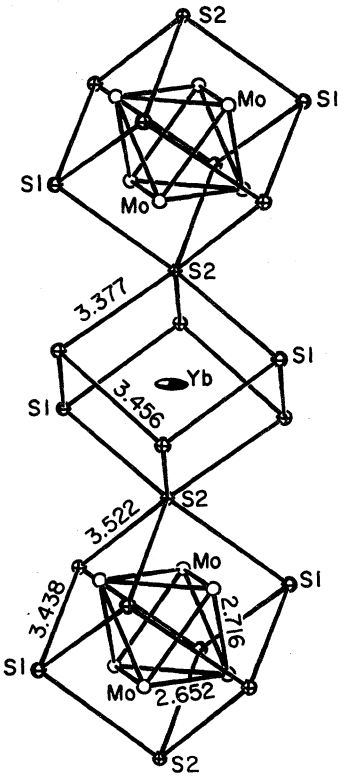

FIG. 1. Partial unit cell of the $YbMo_6S_8$ structure showing the alternating Mo_6S_8 and YbS_8 units along the threefold axis.

Thus the metal ion undergoes strongly anharmonic thermal vibration, possibly even rotational motion, around the origin or around a sixfold set of sites displaced slightly from and centered on the origin.[6] Based on phenomenological models relating the degree of delocalization to the rhombohedral angle α, and measurements of α versus temperature, it has been suggested that the metal ion condenses to the origin at low temperature. However, this hypothesis has not been confirmed by structural refinement at low temperature.

This paper reports ^{170}Yb Mössbauer-effect measurements which show an isomer shift in $YbMo_6S_8$ consistent with pure Yb^{2+}. The anisotropy of the thermal component of the Yb delocalization is evaluated from the Goldanskii-Karyagin effect and compared with the total static and thermal anisotropy obtained from a full structural refinement of neutron powder diffraction data. Structural refinements at 16, 77, and 295 K show the degree of delocalization of Yb and other structural features versus temperature and elucidate the effect of the anisotropic thermal motion of Yb on the thermal expansion.

II. SAMPLE PREPARATION

The $YbMo_6S_8$ samples were synthesized from the elements in fused-silica ampoules. Yb_2S_3 was initially formed from Yb metal (Rare Earth Products Limited, *m* 4*N*, sublimed) and S (Alfa Products, *t* 5*N* 5, lump). The Mo (Atomergic Chemetals Corp., *m* 4*N*, powder) was reduced in a hydrogen stream at 800—900 °C for two days to remove oxygen-containing species. All handling of the materials was done in a nitrogen-filled glove bag.

Because of the large sample size (15 g), the components were not mixed and prereacted in a single tube. An ampoule was made with a constriction which separated the tube into two sections. The Yb_2S_3-Mo mixture and the S were each placed at opposite ends of the tube with a quartz-wool plug at the constriction. The ampoule was evacuated to 5×10^{-7} Torr, sealed-off, and placed in a two-zone furnace. The temperatures of the Yb_2S_3-Mo mixture and the S were held at 700 and 350 °C, respectively. After the S had transported and reacted, the ampoule was heated for two days at 1100 °C. The ampoule was then opened, the prereacted material was well ground with an agate mortar and pestle and placed in another fused-silica tube. This tube was evacuated and then heated for two days at 1350 °C. It was necessary to regrind and refire the material a second time to obtain complete reaction. Two samples were made with starting compositions of $Yb_1Mo_6S_8$ and $Yb_{1.2}Mo_6S_8$.

X-ray diffraction of the $Yb_{1.0}Mo_6S_8$ sample showed two barely detectable impurity peaks with a peak-height intensity less than 0.03 of the 101 Chevrel-phase peak. The position of the impurity peaks indicate Mo_2S_3 and possibly Yb_2O_2S as impurity phases. The neutron-diffraction powder pattern of this sample did not show the above impurities but did have some weak additional peaks which have been tentatively assigned to alpha cristobalite. The $Yb_{1.2}Mo_6S_8$ sample was not single phase. The x-ray diffraction pattern showed many, unidentified impurity peaks and its reaction with 1*N* HCl to evolve H_2S indicated the presence of reactive ytterbium sulfides. Only the $Yb_{1.0}Mo_6S_8$ sample was used for subsequent measurements.

III. RESULTS AND DISCUSSION

A. Mössbauer measurements

The Mössbauer effect of ^{170}Yb in $YbMo_6S_8$ was measured with the use of a monochromatic source of $^{170}TmAl_2$. The 84-keV resonant gamma rays were detected with the use of a scintillation detector supported by fast-counting electronics. The

Mössbauer spectra were collected in a ND6600 computer-based analyzer synchronized with an electromechanical drive operated in the sine-wave mode.

In Fig. 2 we present the Mössbauer spectrum of $YbMo_6S_8$ measured at 4.2 K. Unlike previously reported work[3,4] the spectrum uniquely consists of one quadrupole pattern representing only one type of Yb atom in our sample. The data analysis was performed assuming that the Yb atoms occupy the $\bar{3}$-symmetry position in the sulphur cube. This results in an axially symmetric electric-field-gradient (EFG) tensor which interacts with the quadrupole moment (Q) of the excited state ($I=2$) in ^{170}Yb. The interaction Hamiltonian is given by

$$\mathcal{H}=\frac{e^2q_zQ}{4I(2I-1)}[3\hat{I}_z^2-I(I+1)]\,, \tag{1}$$

where q_z is the principal component of the EFG along the rhombohedral axis. The resulting spectrum is made up of three hyperfine lines located at $6P$, $-3P$, and $-6P$ with intensities of 2, 2, and 1, respectively, and where $P=e^2q_zQ/24$. The analysis showed agreement with line positions; however, the intensities were not well accounted for.

The intensity anomaly in a Mössbauer spectrum can arise from the absorber thickness effects.[9] However, in the present case, both due to dilution (the weight percent of Yb in $YbMo_6S_8$ is 17%) and low Debye temperatures, the absorber was estimated to be well below one absorption length thick, which could not produce detectable intensity distortion.

The other reason for an intensity anomaly is the Goldanskii-Karyagin effect[10] suggested earlier.[4] This arises if there is a lattice vibrational anisotropy described by

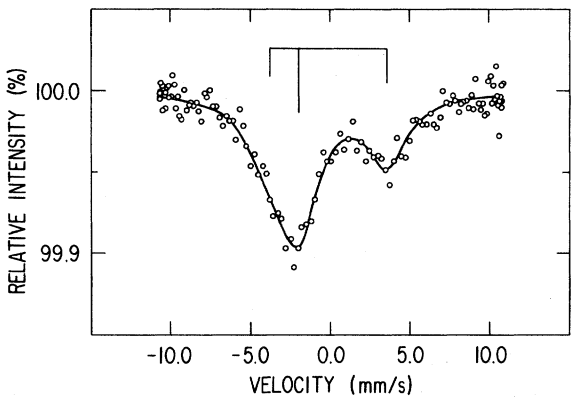

FIG. 2. Mössbauer spectrum of $YbMo_6S_8$ measured with 84-keV resonant gamma transition in ^{170}Yb. The solid line is the least-squares fit to the data discussed in the text. The bar diagram shows the line positions and the intensities (modified by Goldanskii-Karyagin effect) of the quadrupole pattern.

$$f(\theta)=e^{-k^2\langle x_\perp^2\rangle}e^{-\epsilon\cos^2\theta}\,,$$
$$\epsilon=k^2(\langle x_\parallel^2\rangle-\langle x_\perp^2\rangle)\,, \tag{2}$$

where k is the gamma-ray wave vector. The angular dependence of $f(\theta)$ can readily be observed in the quadrupole pattern of a powder sample since it modifies the intensity of a hyperfine transition in comparison to that of an isotropic crystal. A transition with an angular distribution $\Theta_J(\theta)$ will have an intensity

$$I=I_J(\mathrm{CG})^2\,,$$
$$I_J=\int_0^{2\pi}\int_0^{\pi}f(\theta)\Theta_J(\theta)\sin\theta\,d\theta\,d\phi\,, \tag{3}$$

where CG is the appropriate Clebsch-Gordan coefficient.

The analysis of the data can be done by using Eq. (3) and carrying out numerical integrations or by using polynomial expansion procedures.[11] The analysis using a least-squares procedure gave an excellent fit to the data and is shown by the solid line in Fig. 2. The refined parameters are $e^2q_zQ=1000\pm20$ MHz and $\langle x_\parallel^2\rangle-\langle x_\perp^2\rangle=-0.0015\pm0.0001$ Å^2. This result agrees rather well with previous Mössbauer work[3] in spite of the fact that the earlier spectra showed a large component of impurity phase.[4]

The Yb atoms need not occupy the special position with $\bar{3}$ symmetry. Instead, they may be located in the general position displaced off the origin with low-point-group symmetry. This situation demands the use of a quadrupole tensor for which there is no axial symmetry. Hence the x and y components of EFG are not equal. The quadrupole Hamiltonian includes a term related to the asymmetry parameter $\eta=(q_y-q_x)/q_z$. Also the lattice vibrational anisotropy has to be defined more generally through an angular dependence $f(\theta,\phi)$. The introduction of η in the quadrupole Hamiltonian generates five hyperfine lines of equal intensity in the isotropic case.

We have reanalyzed the data using such a Hamiltonian[12] and approximating $f(\theta,\phi)$ by $f(\theta)$. Again a satisfactory least-squares fit was possible with an η of less than 0.3. The lattice anisotropy parameter deduced from this analysis remained almost identical to that obtained with $\eta=0$. The small value of η justifies this approximate analysis and the lack of inherent resolution in the hyperfine lines does not demand any more sophisticated analysis. Hence the conclusion regarding the magnitude of the lattice anisotropy remains unchanged.

The isomer shift given by the analysis is -0.19 ± 0.03 mm/s relative to the $TmAl_2$ source. The different extent of shielding of s electrons by the $4f^{14}$ configuration on Yb^{2+} and the $4f^{13}$ config-

uration on Yb^{3+} should result in different isomer shifts for the two ions. The isomer-shift systematics[13] for Yb shown in Fig. 3 unambiguously show that Yb is divalent in $YbMo_6S_8$.

B. Neutron diffraction

Neutron powder diffraction data were collected on a 12.15-g sample of $YbMo_6S_8$ at 16, 77, and 295 K using the Special Environment Powder Diffractometer (SEPD) at Argonne's Intense Pulsed Neutron Source (IPNS). The sample was contained in a thin-walled ($\sim$0.1-mm) vanadium tube 11.3 mm in diameter and 57.2-mm long and cooled by a closed-cycle Displex (Air Products and Chemicals, Inc.) refrigerator. The SEPD is a time-of-flight powder diffractometer located on a 14-m incident flight path with the capability of placing detectors at any angle from 12°—157° at a constant radius of 1.5 m.[14] For this experiment detectors were positioned in

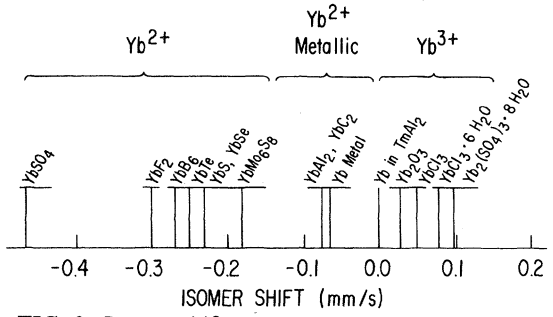

FIG. 3. Isomer-shift systematics for 84-keV Mössbauer resonance in ^{170}Yb. The shift for $YbMo_6S_8$ clearly indicates divalent Yb.

electronically focused groups 10° wide at ±145° and ±90°, 6° wide at ±57°, and 4° wide at ±22°. The high-resolution data ($\Delta d/d \simeq 0.0035$) from the backscattering detectors (±145°) were used for the

TABLE I. Lattice parameters (hexagonal and rhombohedral), unit-cell volume, atomic positions, temperature factors, and weighted profile R values from the refinement of $YbMo_6S_8$ data at 16, 77, and 295 K. Data were refined in space group $R\bar{3}$, No. 148, hexagonal setting.

Parameter	Temperature 16 K	77 K	295 K
a_H (Å)	9.0986(3)	9.1069(3)	9.1449(3)
c_H (Å)	11.3941(2)	11.3912(2)	11.3828(2)
V_H (Å^3)	816.88(8)	818.16(8)	824.40(8)
a_R (Å)	6.4823	6.4856	6.5018
α_R (deg)	89.145	89.189	89.380
x(Yb)	0	0	0
y(Yb)	0	0	0
z(Yb)	0	0	0
β_{11}(Yb)[a]	0.0028(2)	0.0040(2)	0.0054(2)
β_{33}(Yb)	0.000 03(9)	0.0001(1)	0.0008(1)
x(Mo)	0.0172(2)	0.0172(2)	0.0166(2)
y(Mo)	0.1766(2)	0.1763(2)	0.1751(2)
z(Mo)	0.4014(1)	0.4015(1)	0.4015(1)
B(Mo) (Å^2)	0.20(3)	0.25(3)	0.57(4)
x(S$_1$)	0.3329(3)	0.3327(4)	0.3324(4)
y(S$_1$)	0.2907(4)	0.2911(4)	0.2916(4)
z(S$_1$)	0.4168(2)	0.4169(2)	0.4169(3)
B(S$_1$) (Å^2)	0.20(4)	0.26(4)	0.71(5)
x(S$_2$)	0	0	0
y(S$_2$)	0	0	0
z(S$_2$)	0.2389(4)	0.2384(4)	0.2378(4)
B(S$_2$) (Å^2)	0.17(7)	0.20(7)	0.52(9)
R_{wp}(%)	4.040	3.945	3.654

[a]For Yb, $\beta_{11}=\beta_{22}=2\beta_{12}$ and $\beta_{13}=\beta_{23}=0$ where the thermal factor is given by $\exp[-(\beta_{11}h^2+\beta_{22}k^2+\beta_{33}l^2+2\beta_{12}hk+2\beta_{13}hl+2\beta_{23}kl)]$.

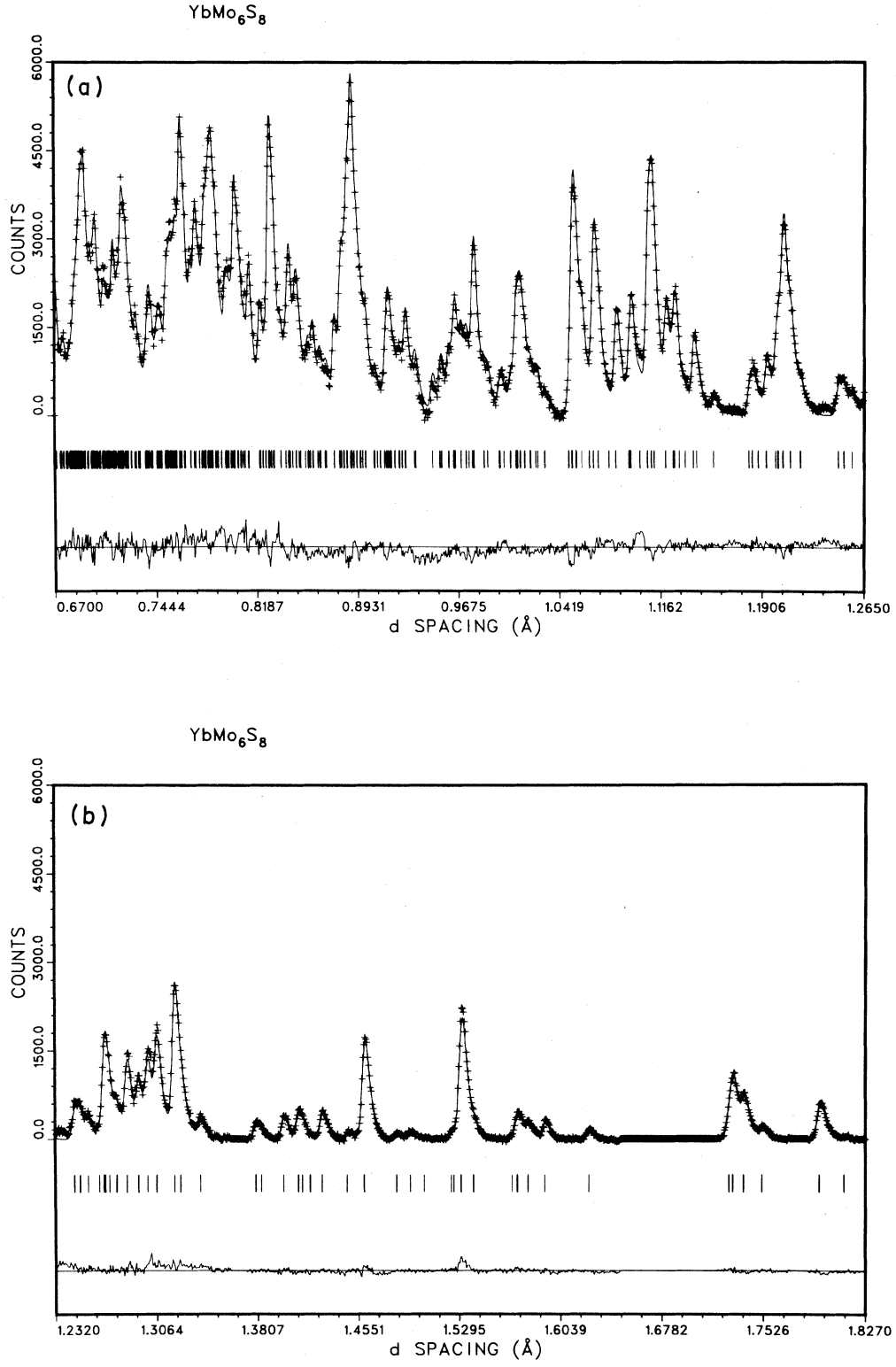

FIG. 4. Rietveld refinement profile for $YbMo_6S_8$ at 295 K showing the raw data (+) and calculated profile (continuous line). Tick marks below the profile mark the positions of all allowed reflections. A difference plot (observed minus calculated) appears at the bottom. Background has been subtracted before plotting.

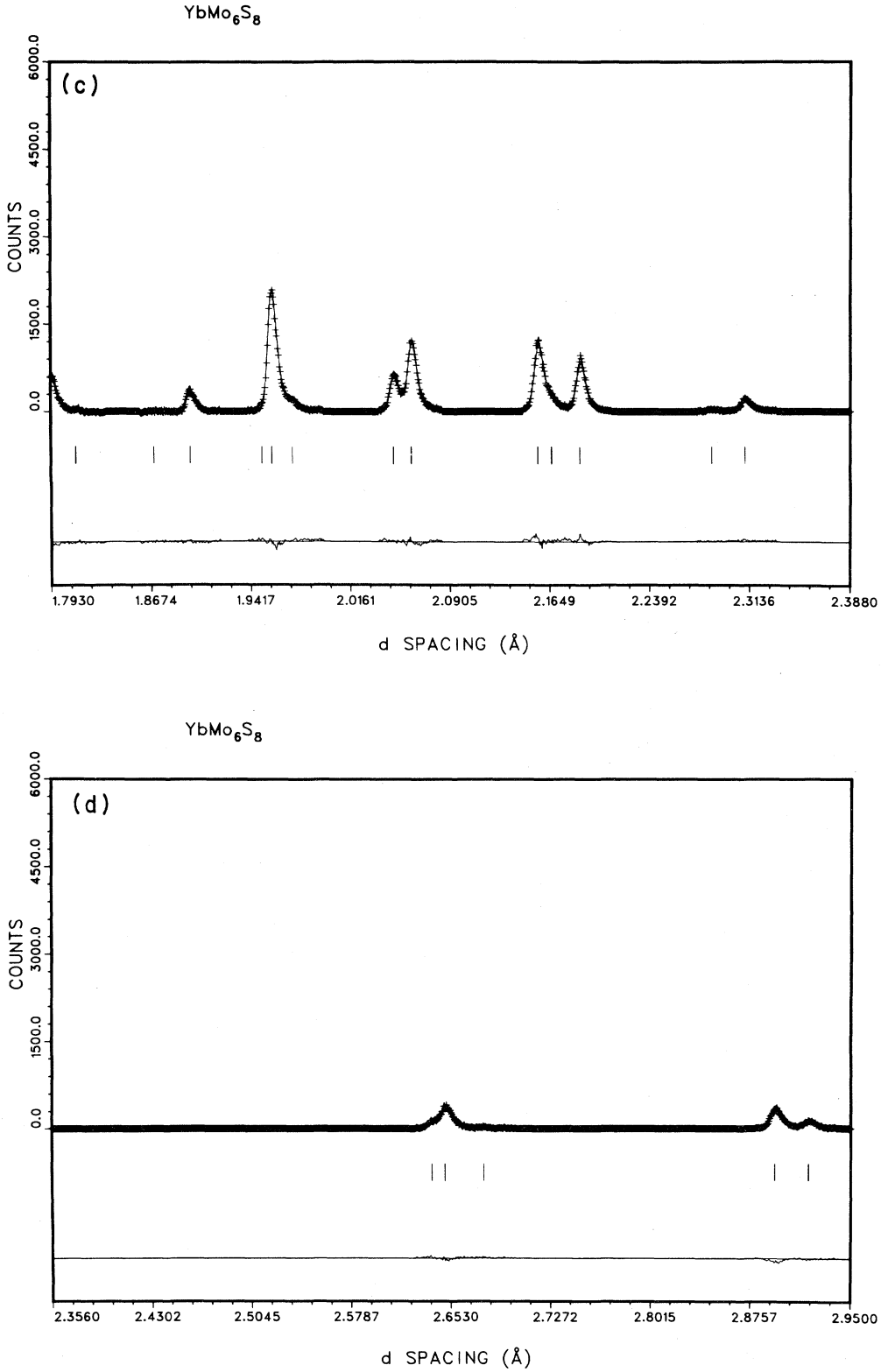

FIG. 4. (*Continued.*)

TABLE II. Refined atomic position and isotropic temperature factor for Yb from a model in which Yb is placed in an $(x,x,0)$ site (hexagonal setting) with an isotropic temperature factor.

Parameter	Temperature 16 K	77 K	295 K
x(Yb)	0.0137(6)	0.0161(6)	0.0244(4)
B(Yb) (Å^2)	0.03(5)	0.07(5)	0.45(7)
R_{wp}	4.044	3.950	3.654

structural refinement. The lower-angle data extend to larger d spacings and allow impurity phases to be identified. No evidence for significant impurity phases was seen in the neutron data.

The diffraction data were refined in hexagonal space group $R\bar{3}$ using the Rietveld method modified for time-of-flight data from pulsed neutron sources.[15,16] The variables in the refinements were the hexagonal lattice parameters a and c, atom positions and isotropic temperature factors for Mo, S_1, and S_2, components of the anisotropic thermal tensor for Yb, a Gaussian peak broadening parameter, extinction and absorption coefficients, and two background parameters. The decision to allow an anisotropic temperature factor only for Yb was made based on significance ratio tests. A model in which the occupancy of Yb at the origin was refined gave n(Yb)=1.01(1). Thus full occupancy was assumed in subsequent analysis. The final refinement profile at 295 K is shown in Fig. 4. Refined parameters and the weighted profile R values at the three temperatures are listed in Table I.

In a model with Yb located at the origin, the apparent thermal anisotropy is pronounced and remains large at low temperatures. In particular, the large value for β_{11} at 16 K suggests that part of the Yb displacement may be static. Thus a second refinement model was tried in which Yb was displaced off the threefold axis into an $(x,x,0)$ position

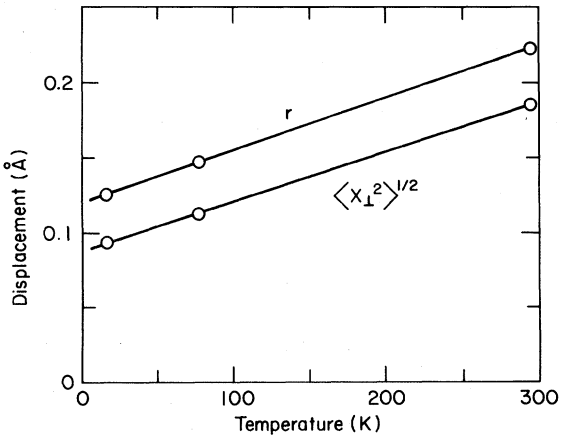

FIG. 5. Perpendicular displacement of Yb from the threefold axis vs temperature as determined from an anisotropic temperature factor model ($\langle x_\perp^2 \rangle^{1/2}$) and a static displacement model (r).

with an isotropic temperature factor. This model disorders the Yb into a planar ring of six sites displaced a distance xa from the origin and has the same number of refineable parameters as the first model. (Thus R values can be compared directly.) The values for x and B(Yb) and the weighted profile R values obtained with this model are in Table II. The R values are identical at 295 K and only slightly larger for the static displacement model at 77 and 16 K, indicating that either model gives a good fit to the data. As expected, from comparison of models alone it is impossible to conclude whether the Yb displacement has a static component.

C. Discussion

The temperature dependence of the root-mean-square thermal displacements perpendicular and

TABLE III. Root-mean-square displacements of Yb perpendicular and parallel to the threefold axis for the model in which Yb is assigned a harmonic, anisotropic temperature factor with Yb at the origin and static displacement of Yb from the origin for the model in which Yb is assigned an isotropic temperature factor and allowed to randomly occupy a sixfold set of sites displaced from the origin.

	Temperature 16 K	77 K	295 K
	Anisotropic temperature factor model		
$\langle x_\perp^2 \rangle^{1/2}$ (Å)	0.094(3)	0.112(3)	0.185(3)
$\langle x_\parallel^2 \rangle^{1/2}$ (Å)	0.014(21)	0.025(13)	0.074(6)
	Static displacement model		
r (Å)	0.125(5)	0.147(5)	0.223(4)

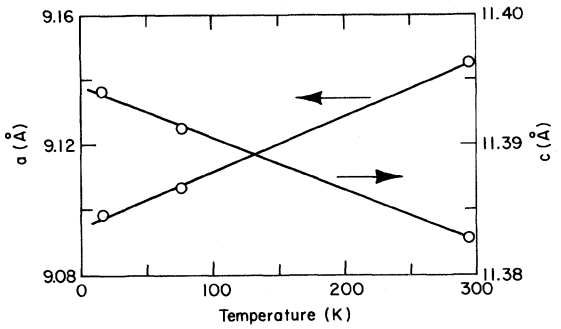

FIG. 6. Temperature dependence of the hexagonal lattice parameters a and c in $YbMo_6S_8$.

parallel to the threefold axis ($\langle x_\perp^2\rangle^{1/2}$ and $\langle x_{||}^2\rangle^{1/2}$) and the static displacement ($r = xa$) are compared in Table III, and the perpendicular components are plotted in Fig. 5. The magnitude of the displacement depends on the model. However, both show the same temperature dependence and indicate that a significant displacement remains at 16 K: 0.094(3) Å for the thermal model or 0.125(5) Å for the static model. The anisotropy at 16 K from the diffraction result is

$$\langle x_{||}^2\rangle - \langle x_\perp^2\rangle = -0.0086 \pm 0.0008 ,$$

measured in units of Å^2. Extrapolating to 4 K changes the result only slightly. This is substantially larger than the anisotropy obtained from the Goldanskii-Karyagin effect (-0.0015 Å^2) and indicates that a significant static displacement must be present.

The thermal expansion of $YbMo_6S_8$ is very anisotropic. As shown in Fig. 6 the c axis actually expands upon cooling. The cause of this anisotropy, as well as other interesting structural features, can be understood by examining atom-atom distances versus temperature (Table IV). As the temperature decreases Yb attempts to condense to the high-symmetry point at the origin. Since the Yb-S_2 distances are already uncomfortably short, the S_2-S_2 distance through the origin increases as temperature decreases. This increase is large enough to offset the decrease in S_2-S_2 distance through the Mo_6 octahedron and result in an overall expansion along c.

A second unusual effect observed is the expansion of Mo—Mo bonds within the Mo octahedra as temperature decreases. In spite of the overall cell elongation along c, all of the S-S distances in the network contract as temperature decreases. All five Mo—S bonds, including the exobond to a sulfur of a neighboring Mo_6S_8 unit, contract at roughly the same rate. This contraction of Mo—S bonds is accompanied by an elongation of Mo—Mo bonds and results in a significant decrease (0.03 Å) in the Mo-Mo intercluster distance at 16 K.

IV. CONCLUSIONS

A single phase sample was synthesized with stoichiometry $YbMo_6S_8$. Structural refinement

TABLE IV. Comparison of interatomic distances (Å) in $YbMo_6S_8$ at 16, 77, and 295 K.

Atoms	Temperature 16 K	77 K	295 K
Mo_6S_8 cube			
Mo-Mo	2.658(2)	2.655(2)	2.652(3)
Mo-Mo	2.721(2)	2.719(2)	2.716(2)
Mo-Mo (intercluster)	3.190(2)	3.196(2)	3.221(3)
S_1-S_1	3.429(3)	3.430(3)	3.438(4)
S_1-S_2	3.503(4)	3.508(4)	3.522(4)
S_2-S_2 (via Mo_6)	5.950(6)	5.959(6)	5.969(7)
Mo-S_1	2.439(3)	2.444(3)	2.454(4)
Mo-S_1	2.458(3)	2.459(3)	2.464(3)
Mo-S_1	2.525(3)	2.525(3)	2.536(4)
Mo-S_1 (exo)	2.563(3)	2.565(3)	2.571(3)
Mo-S_2	2.405(4)	2.408(4)	2.411(4)
Mo-S (average)	2.478	2.480	2.487
YbS_8 cube			
Yb-S_1	3.017(3)	3.022(3)	3.039(3)
Yb-S_2	2.722(4)	2.716(4)	2.707(5)
S_1-S_1	3.436(3)	3.441(3)	3.456(4)
S_1-S_2	3.367(3)	3.368(3)	3.377(4)
S_2-S_2 (via Yb)	5.444(6)	5.432(6)	5.414(7)

shows the Yb position at the origin to be fully occupied. The ^{170}Yb Mössbauer spectrum exhibits a single site with an isomer shift consistent with Yb^{2+}. Comparing the anisotropy of the thermal vibration obtained from the Mössbauer measurements with the overall "delocalization" from neutron-diffraction structural refinements suggests that significant static delocalization is present even at low temperatures. Thus the equilibrium site for Yb may actually be a site of general symmetry rather than the special position at the origin normally assumed. This possibility should be considered in the interpretation of any data which probes the local Yb environment or near-neighbor distances around Yb. The same situation undoubtedly exists in other Chevrel-phase structures.

ACKNOWLEDGMENT

This work was supported by the U.S. Department of Energy.

---

*On leave from the Instituto de Fisica, UFRGS, Porto Alegre, Brazil.

[1]Ø. Fischer, A. Treyvand, R. Chevrel, and M. Sergent, Solid State Commun. 17, 721 (1975).

[2]N. E. Alekseevskii, G. Wolf, K. Bohmhammel, N. M. Dobrovolskii, and C. Hohlfeld, Phys. Status Solidi A 51, 399 (1979).

[3]P. Bonville, J. A. Hodges, P. Imbert, G. Jehanno, R. Chevrel, and M. Sergent, Rev. Phys. Appl. 15, 1139 (1980).

[4]P. Bonville, R. Chevrel, J. A. Hodges, P. Imbert, G. Jehanno, and M. Sergent, in Proceedings of the International Conference on Application of the Mössbauer Effect, Jaipur, India, 1981 (in press).

[5]J.-M. Tarascon, D. C. Johnson, and M. J. Sienko, Inorg. Chem. 21, 1505 (1982).

[6]K. Yvon, in *Current Topics in Materials Science,* edited by E. Kaldis (North-Holland, Amsterdam, 1979), Vol. 3, Chap. 2, and the references cited therein.

[7]J. D. Jorgensen, D. G. Hinks, and F. J. Rotella, in *Ternary Superconductors,* edited by G. K. Shenoy, B. D. Dunlap, and F. Y. Fradin (Elsevier, Amsterdam, 1981), p. 69.

[8]K. Yvon, Solid State Commun. 25, 327 (1978).

[9]G. K. Shenoy, J. M. Friedt, H. Maletta, and S. L. Ruby, in *Mössbauer Effect Methodology,* edited by J. J. Gruveramn, C. W. Seidel, and D. K. Dieterly (Plenum, New York, 1974), Vol. 8, p. 277.

[10]V. I. Goldanskii *et al.*, Dok. Akad. Nauk. SSSR 147, 127 (1962); S. V. Karyagin, Dok. Akad. Nauk. SSSR 148, 1102 (1963).

[11]G. K. Shenoy and J. M. Friedt, Nucl. Instrum. Methods 136, 569 (1976).

[12]G. K. Shenoy and B. D. Dunlap, Nucl. Instrum. Methods 71, 285 (1969).

[13]E. R. Bauminger, G. M. Kalvius, and I. Nowik, in *Mössbauer Isomer Shifts,* edited by G. K. Shenoy and F. E. Wagner (North-Holland, Amsterdam, 1978), p. 661.

[14]B. S. Brown, J. M. Carpenter, J. D. Jorgensen, and D. L. Price, in *Novel Materials and Techniques in Condensed Matter Physics,* edited by G. Crabtree and P. Vashishta (Elsevier, Amsterdam, 1982), p. 311.

[15]J. D. Jorgensen and F. J. Rotella, J. Appl. Crystallogr. 15, 27 (1982).

[16]R. B. Von Dreele, J. D. Jorgensen, and C. G. Windsor, J. Appl. Crystallogr. 15, 581 (1982).